AIAA 2001-4305

ADJUSTABLE LIMITING ALGORITHMS FOR ROBUST MOTION SIMULATION

R. E. McFarland*

NASA, AMES Research Center, Moffett Field, CA 94035-1000 USA

Abstract

Motion-based aircraft simulators use washout filters to suppress sustained motion. However, these filters occasionally produce dynamics requiring assistance from limiting algorithms to constrain a simulator to electrical and physical limits. These limiting algorithms should minimally interfere with "normal simulator operations" using washout filters, while ensuring that physical and electrical boundaries are not transcended. In addition, these algorithms should provide an adjustable relationship between efficiency during normal operations and comfort during limiting. Under the assumption that limiting is implemented using linear, second order filters, all coefficients may be determined by the selection of a single normalized parameter per axis, along with the axis' hard limits. The relationships that unify washout and limiting filters are called "Adjustable Limiting Algorithms for Robust Motion Simulation" (ALARMS). These algorithms produce a robust interface while establishing efficiency metrics for motion cues relative to the maximum capacity of a simulator.

I. Introduction

To control a motion simulator, two distinct regions of command activity are defined. The "normal region" is where the aircraft states are emulated by onset cues. This region (in which washout filters are active) is called the "region of unrestricted travel excursions," or ROUTE. Commands are issued from the mathematical model as functions of pilot control activity and filters "wash out" sustained motion while producing onset cues. For each axis these washout filters are tuned in accordance with the task, simulator limitations, and physiological considerations. Washout filters represent an effective technology for providing cues to pilots, because simulators typically have very restrictive hard limits.

The intrusive limiting region is the secondary region of control activity, where the only concerns are the safety and comfort of the pilot, and prevention of damage to the motion system. In this region, algorithms are activated that ignore pilot commands and aircraft dynamics because electrical or physical boundaries are threatened. In the most idyllic of situations in terms of comfort, the pilot would be unaware that authority had been usurped by autonomous control functions. But, motion responses are disassociated from pilot inputs during limiting and increased pilot comfort requires the dedication of a large amount of simulator capacity to limiting operations. Hence, the limiting region should be as small as possible in conformance with the hard motion limits of a particular simulator, but large enough to provide sufficient dedicated capacity for a selected level of pilot comfort during limiting.

As the washout region is increased, the limiting region is decreased. The restorative dynamics required by limiting functions then become larger, and hence more noticeable by the pilot, when they occur. The system that controls limiting is called "ALARMS," an acronym for the title of this paper.

The most intrusive limiting technique within the capacity of a motion system is that where constant, maximum deceleration is applied, beginning at an appropriate activation point. This technique is called "parabolic limiting." Although it permits the greatest possible ROUTE, it is not acceptable as a general limiting algorithm because its application invariably terminates a simulation experiment. The resultant motion cues are well above pilot perception levels, and are uncomfortable.

As a compromise, the simulation community accepts the imposition of filtered behavior during limiting, where the filters are generally linear and second order. Compared to parabolic limiting, second order filters require the dedication of more simulator capacity to the limiting phenomenon, and thus produce less intrusive pilot cues.

---

* *Research Engineer, Aerospace Simulation Operations Branch, Senior Member AIAA*

II. Performance Parameter

Motion simulator efficiency relative to limiting has not been previously quantified. Washout and limiting regions are here developed as functions of a single normalized parameter *P*, which quantifies the aggressiveness of limiting. It also produces an efficiency metric for each axis. This is accomplished by defining a "relative volume" with respect to the maximum capacity of a simulator. Each axis is treated independently, so this is not the physical volume[1] or "workspace"[2,3] of the simulator. The efficiency metric is the percentage of the maximum ROUTE that is available, for a given value of the parameter *P*, relative to the maximum capacity of the simulator. It does not quantify how efficiently a washout filter utilizes the available ROUTE.

All the required coefficients for limiting algorithms are determined by the selection of the parameter, which simultaneously establishes both the efficiency of the motion simulator in utilizing its available real estate for normal simulator operations and pilot comfort level during limiting. "Normal simulator operations" are defined as motion operations (using washout filters) where data are generated without contamination by false motion cues due to limiting. The adjustable parameter lies in the range,

$$0 \le P \le 1 \tag{1}$$

At the upper limit of this parameter the filters permit maximum simulator performance under washout filter control, while reducing pilot comfort when limits are encountered. At the lower limit the converse is true. The available range with respect to recovery dynamics is bounded as follows: For *P*=1 the simulator can briefly achieve its hard acceleration limit during a limiting process. For P=0 the arbitrary level of one-half the acceleration limit during limiting dynamics is the maximum that can be achieved.

III. ROUTE as a Volume

For a given simulator axis it is useful to think of the position-velocity-acceleration product ($u\dot{u}\ddot{u}$) as a volume, where "u" is a generalized translational or rotational axis. This permits the establishment of a metric for the efficiency of the motion system in terms of the ROUTE for each axis of the simulator as compared to its maximum capacity. NASA's Vertical Motion Simulator (VMS) has the largest available range for research into motion control and limiting procedures, and its motion may be scaled to investigate limits in simulators with less capacity. Numerical examples used here for illustrative purposes are representative the vertical axis ($u \to z$) of the VMS, where the positive quadrant hard limits selected for this study are $z_L = 22$ ft, $\dot{z}_L = 15$ ft/sec, and $\ddot{z}_L = 22$ ft/sec^2.

For an arbitrary axis, considering all eight quadrants of simulator motion in a "volume" with axes ($u, \dot{u}, \ddot{u}$), the theoretically maximum ROUTE is $8\,u_L\dot{u}_L\ddot{u}_L$ (excursions may be either positive or negative). This volume is not attainable because activation of parabolic limiting occurs on the locus of points given by,

$$\dot{u}^2 = 2\ddot{u}_L\left(u_L - |u|\right) \tag{2}$$

This equation is obtained by assuming that the constant acceleration limit applies until the simulator comes to rest at the position limit. For normalization purposes the maximum available volume must thus be reduced from a cube to that attainable using the parabolic limiting algorithm. This represents an approximate 4% decrease. The "volume" defining the maximum simulator capacity becomes,

$$V_p = 8u_L\dot{u}_L\ddot{u}_L\left(1 - \frac{\dot{u}_L^2}{12u_L\ddot{u}_L}\right) \tag{3}$$

This volume is shown in Fig. 1 for the vertical axis, where the generalized variable "*u*" becomes "*z*". The indicated velocity-versus-position limitation applies only during approaches to a hard position limit (where both velocity and position have the same sign), so the volume has symmetry. The conditions for the onset of parabolic responses are independent of the current acceleration, which upon activation is instantaneously limited ($\pm\ddot{z}_L$).

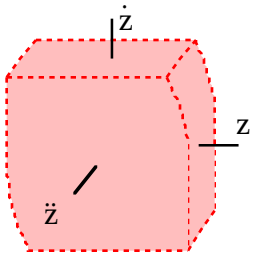

Fig. 1 – Parabolic Volume, Vertical Axis

The "constant deceleration at the limit" of parabolic limiting would be an uncomfortable situation for pilots, and its onset would produce an undesirable jerk to the motion system. Parabolic limiting is therefore avoided, although it establishes the baseline ROUTE from which the efficiencies of other algorithms are measured. The relative efficiency of other algorithms can therefore approach, but never achieve 100%. ALARMS produces volumes (and hence, efficiencies) that are functions of the parameter *P*; less intrusive than parabolic limiting.

IV. Washout Filters

The translational and rotational inputs to washout filters are the desired accelerations of the motion simulator, as developed by the aircraft model in response to pilot inputs and simulated phenomena, such as atmospheric disturbances and runway encounters. Besides vehicle dynamics, these inputs account for scaling, cross coupling, induced effects, and other special features of a motion system such as residual tilt. The desired simulator "high pass" acceleration commands are not discussed here, but it should be recognized that behavior beyond the capacity of the motion simulator may be requested, even when this behavior is "washed out" by second-order filters. The washout filters may themselves be modified "continuously according to the aircraft input and simulator states."[4]

For any degree of freedom the input "$\ddot{x}$" is applied to a low pass filter, where the input is a combinatorial function of aircraft states in response to pilot inputs. Using a Laplace mathematical form, the motion system states are computed from,

$$u(s) = \frac{\ddot{x}(s)}{s^2 + a_2 s + a_1} \tag{4}$$

Washout filters suppress sustained motion as well as provide onset cues, but they occasionally require assistance in constraining jerk, acceleration, velocity, and position to prescribed limits. When this occurs, pilot inputs and the washout filter outputs are ignored. Therefore, in the limiting region all motion cues are false.

V. Regions

The combination of the ROUTE for normal simulation operations and the region required for limiting constitutes the entire available capacity of a motion simulator. Increasing the size of one region decreases the other. The limiting region may be quantified and constrained to adjustable levels because the mathematical description of limiting dynamics may be controlled by a single parameter, per axis. In contrast, behavior in the ROUTE is at the discretion of the researcher, who specifies the washout coefficients.

The limiting region must be sufficient to constrain all states to their limits for all "onset" conditions, and do so with an adjustable level of aggressiveness, independent of motion system dynamics in the ROUTE. This design objective defines an envelope of states where the activation of the limiting algorithms must occur.

The magnitude of possible motion cues during limiting should range from barely noticeable to intrusive, because researchers have considerable philosophical differences about their importance (which also has some dependence on the task). Whereas one researcher may want to terminate data-gathering operations when limiting occurs, another researcher may desire ameliorated motion cues during limiting such that experimentation is not interrupted. The intensity of limiting cues should therefore be adjustable. Correspondingly, if limiting is intrusive a large ROUTE is available for normal simulation operations, decreasing the probability that limits will be encountered. If limiting is adjusted to be not very noticeable then a smaller ROUTE is available for normal simulation operations, and the probability of encountering the limiting phenomenon is greater.

Hard limits are defined for each degree of freedom of a simulator, here generalized to ($u_L, \dot{u}_L, \ddot{u}_L, \dddot{u}_L$). The position, velocity and acceleration limits are specified, but the jerk limit $\dddot{u}_L$ is computed by unifying the dynamics of the velocity and position limiting algorithms. The jerk limit is well defined for position limiting, but unbounded for either washout filtering or velocity limiting. By specifying that the maximum jerk cannot exceed that which occurs during the selected, most aggressive instance of position limiting, the limiting operations are unified and become a function of the parameter *P*.

During limiting operations, limiting motion cues to small magnitudes requires the dedication of a large amount of simulator real estate to limiting operations, whereas large limiting cues do not require as much. Also, limiting dynamics and washout filter coefficients are independent; the boundary of the ROUTE determines the dynamics during limiting. A relationship thus exists where "normal operations" are more efficient if limiting is intrusive. If the maximum capacity of a simulator is required for a particular experiment, then very little real estate is available for limiting. But, when limiting occurs, it would be intrusive. If less simulator capacity is tolerable, then more real estate may be dedicated to limiting. In this case, when limiting occurs it is less intrusive.

VI. Jerk and Acceleration Limiting

Limits on jerk and acceleration are initially accommodated using the washout filters themselves, by implementing a pseudo command technique in which states are re-computed to deliver all washout outputs that obey the constraints. Acceleration ($\ddot{u}$) is clamped to its hard limit ($\ddot{u}_L$), and the jerk is constrained to its hard limit ($\dddot{u}_L$), later defined, by adjusting acceleration. For example, the jerk from a washout filter is approximated in a discrete model by a difference equation which uses the cycle time "*h*" and the current and previous acceleration,

$$\dddot{u}_k \approx \left(\ddot{u}_k - \ddot{u}_{k-1}\right)/h \tag{5}$$

If the approximated jerk is greater than its hard limit "$\dddot{u}_L$", it is set equal to the hard limit and the acceleration is adjusted to reflect this substitution:

$$\ddot{u}_k = \begin{cases} \ddot{u}_{k-1} + h\dddot{u}_L \operatorname{sgn}(\dddot{u}_k) & \text{if } |\dddot{u}_k| > \dddot{u}_L \\ \ddot{u}_k & \text{otherwise} \end{cases} \quad (6)$$

And if the acceleration is greater than its hard limit, it is clamped to the hard acceleration limit "$\ddot{u}_L$".

$$\ddot{u}_k = \begin{cases} \ddot{u}_L \operatorname{sgn}(\ddot{u}_k) & \text{if } |\ddot{u}_k| > \ddot{u}_L \\ \ddot{u}_k & \text{otherwise} \end{cases} \quad (7)$$

If acceleration is modified in this sequence, the position and velocity states ($u, \dot{u}$) are re-computed to conform to the dynamics of the washout filter.

VII. Position Limiting

If position limiting is activated, a specific second-order differential equation controls the motion responses. It is critically damped to avoid position overshoot, has a constant input of the position limit u_L, and its single coefficient is the natural frequency ω of the limiting filter, which cannot exceed a maximum value. The natural frequency is linearly related to the maximum acceleration that can occur during position limiting, or "recovery," such that this relationship establishes the maximum value. The position-limiting filter is given by,

$$u(s) = \frac{\omega^2 u_L \operatorname{sgn}(\ddot{x})}{(s+\omega)^2} \quad (8)$$

Limiting must be activated at the pertinent states of a trajectory. The determination of these states is based upon predicted performance under the control of the limiting filters, independent of the origin of the states themselves.

An important step in establishing the proper limiting trajectories is to select the natural frequency for use in the position-limiting differential equation.

$$\omega = \tfrac{1}{2}(1+P)\frac{e\ddot{u}_L}{\dot{u}_L} \quad (9)$$

The range of viable frequencies is to a maximum point, beyond which the "recovery deceleration" could violate its hard limit $\ddot{u}_L$. Arbitrarily, the minimum natural frequency is selected to be one-half this value. This lower limit may be adjusted if accrued experience determines that "non-intrusive" limiting requires a modification. With Equation (9) defining the natural frequency, during position limiting the recovery acceleration is limited by,

$$|\ddot{u}| \le \tfrac{1}{2}(1+P)\ddot{u}_L \quad (10)$$

This is demonstrated in the next two figures. In Fig. 2 the passive case of P=0 is shown, where the recovery acceleration achieves half of the maximum deceleration (11 ft/sec^2), as predicted in Equation (10). This only occurs when the initial velocity is at the limit, however, because smaller initial velocities produce less aggressive limiting dynamics. Equally spaced parametric curves are presented representing the full range of the velocity of activation.

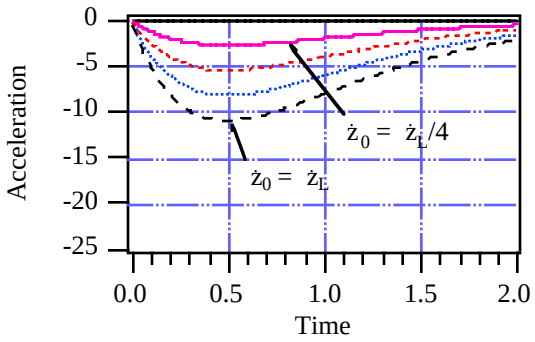

Fig. 2 – Recovery Accelerations, P=0

In Fig. 3 the aggressive case of P=1 is shown, where the recovery acceleration achieves the maximum deceleration (22 ft/sec^2) when the initial velocity is at the limit. This is given by the bottom dashed line in Fig. 3.

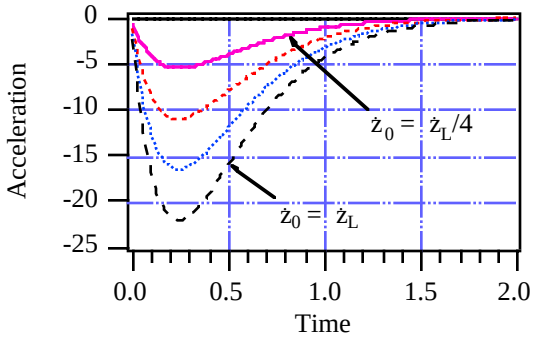

Fig. 3 – Recovery Accelerations, P=1

These limited dynamics occur because the recovery acceleration obeys the inequality,

$$|\ddot{u}| \le \omega \dot{u}_L e^{-1} \quad (11)$$

Equations (9) through (11) are produced by examining the extreme state values that will occur under the control of Equation (8). This is accomplished by activating Equation (8) at unique states that are themselves computed by curtailing the maximums to the motion system's hard limits.

During the recoveries of Figs. 2 and 3 the velocity versus position relationships are as shown in Figs. 4 and 5.

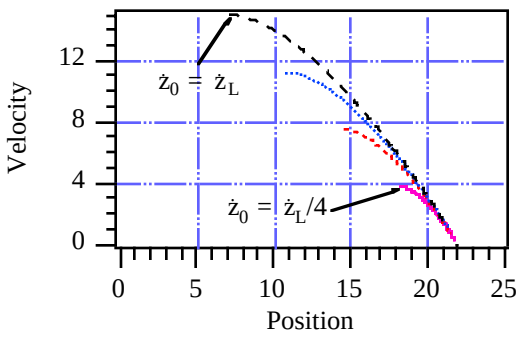

Fig. 4 – States, *P*=0

Fig. 4 represents the "minimum efficiency" case because for *P*=0 the limiting phenomenon restricts the ROUTE most. (The ROUTE for each example is the region to the left of the recovery trajectories). In contrast, the case of *P*=1 in Fig. 5 represents the "maximum efficiency" case because the ROUTE is maximum.

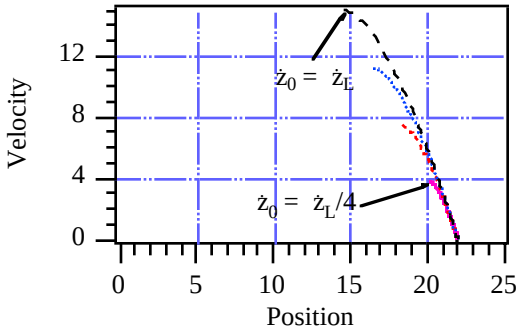

Fig. 5 - States, *P*=1

Figs. 4 and 5 demonstrate that the function controlling the onset of position limiting may be adjusted to curtail the recovery dynamics by use of the parameter *P*. Velocity limiting is linked to this process through the maximum jerk.

The initially null accelerations of Figs. 2 and 3 produce the velocity versus position trajectories of Figs. 4 and 5. Note that the ROUTE is smaller for smaller *P*. At any initial acceleration the velocity and position at activation (subscript "zero") conform to the relationship,

$$\pm\omega^2 u_L = \omega^2 u_0 + 2\omega\dot{u}_0 + \ddot{u}_0 \tag{12}$$

This is simply the position limiting differential equation at its point of activation. As functions of time from activation the states may be written in closed form:

$$\begin{aligned} u(t) &= u_0 - \frac{1}{\omega}\left(\ddot{u}_0 + \omega\dot{u}_0\right)te^{-\omega t} + \frac{1}{\omega^2}\left(\ddot{u}_0 + 2\omega\dot{u}_0\right)\left(1 - e^{-\omega t}\right) \\ \dot{u}(t) &= \left[\dot{u}_0 + \left(\ddot{u}_0 + \omega\dot{u}_0\right)t\right]e^{-\omega t} \\ \ddot{u}(t) &= \left[\ddot{u}_0 - \omega\left(\ddot{u}_0 + \omega\dot{u}_0\right)t\right]e^{-\omega t} \\ \dddot{u}(t) &= \omega\left[-\left(2\ddot{u}_0 + \omega\dot{u}_0\right) + \omega\left(\ddot{u}_0 + \omega\dot{u}_0\right)t\right]e^{-\omega t} \end{aligned} \tag{13}$$

These equations are used to obtain the restriction on natural frequency, and to define the locus of activation points for position limiting. Activation states depend upon maximum and minimum values for these equations, where both finite-time and asymptotic final value solutions must be considered.

VIII. Velocity Limiting and Activation

If velocity limiting is active, another second order differential equation controls the motion responses. It also has a constant input and a single parameter.

$$u(s) = \frac{\dot{u}_L \operatorname{sgn}(\dot{u})}{s(\tau_v s + 1)} = \frac{k_v \dot{u}_L \operatorname{sgn}(\dot{u})}{s(s + k_v)} \tag{14}$$

This differential equation smoothly constrains velocity to the hard limit $\dot{u}_L$. As a function of acceleration, velocity is constrained to approach (not when retreating from) its hard limit as an exponential function of time from activation. An exponential decay of velocity in time is equivalent to a linear decay of acceleration with respect to velocity, as is diagrammed in Fig. 6.

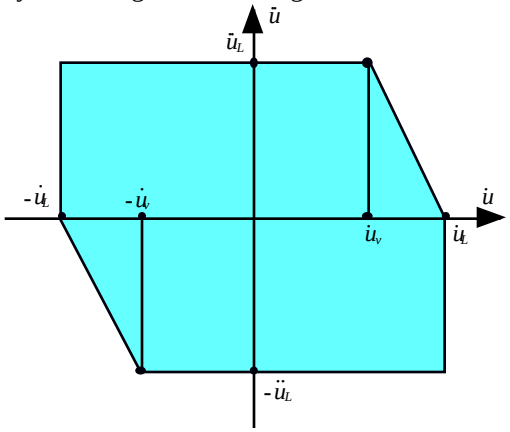

Fig. 6 – Acceleration vs. Velocity Limits

From Fig. 6 the time constant and coefficient in Equation (14) are computed from a velocity breakpoint "$\dot{u}_v$".

$$\tau_v = k_v^{-1} = \frac{\dot{u}_L - \dot{u}_v}{\ddot{u}_L} \tag{15}$$

The activation of velocity limiting depends upon a dummy variable "ψ," where,

$$\psi = \ddot{u} + k_v\dot{u} \tag{16}$$

The velocity-limiting algorithm must be applied whenever $|\psi| \geq k_v \dot{u}_L$.

During velocity limiting the jerk is,

$$\dddot{u} = -k_v \ddot{u} = -\frac{\dddot{u}\ddot{u}_L}{\dot{u}_L - \dot{u}_v} \tag{17}$$

Hence, the maximum value of jerk due to velocity limiting is a function of the breakpoint velocity $\dot{u}_v$,

$$\dddot{u}_L = \frac{\ddot{u}_L^2}{\dot{u}_L - \dot{u}_v} \tag{18}$$

Jerk becomes unbounded as the breakpoint velocity approaches the hard velocity limit, so a limit must be placed on this quantity. By equating this limit to the maximum jerk that can be developed during position limiting using the parameter *P* (as well as the maximum jerk permitted by the washout filters), all the regions are unified.

During position limiting the jerk is bounded, and given by,

$$\dddot{u} = -\omega(\omega\dot{u} + 2\ddot{u}) \tag{19}$$

Since acceleration decreases for velocities beyond the velocity breakpoint (see Fig. 6), the maximum magnitude of jerk due to position limiting is given by,

$$\dddot{u}_L = \omega(\omega\,\dot{u}_v + 2\ddot{u}_L) \tag{20}$$

The maximum jerks from both velocity and position limiting are equated to produce the jerk limit,

$$\dddot{u}_L = \omega\,\ddot{u}_L + \frac{\omega^2 \dot{u}_L}{2}\left[1 + \sqrt{1 + \frac{4\ddot{u}_L}{\omega\,\dot{u}_L}}\right] \tag{21}$$

Similarly, the velocity breakpoint is given by,

$$\dot{u}_v = \dot{u}_L - \frac{\ddot{u}_L^2}{\dddot{u}_L} = \frac{\dot{u}_L}{2}\left(1 + \sqrt{1 + \frac{4\ddot{u}_L}{\omega\dot{u}_L}}\right) - \frac{\ddot{u}_L}{\omega} \tag{22}$$

The conditions for the activation of position limiting are given below.

IX. Position Limit Activation

The required dummy variables for the determination of whether the position limiting differential equation should be activated are,

$$\gamma = u + \frac{\dot{u}}{\omega}$$
$$\beta = \frac{\dot{u}}{\omega} + \frac{\ddot{u}}{\omega^2} \tag{23}$$

$$\alpha = \begin{cases} \gamma + \beta & |\gamma| \leq u_L \text{ or } \dot{u}\beta \geq 0 \\ \gamma + \beta\left[1 - \exp\left(\dfrac{\dot{u}}{\omega\beta}\right)\right] & |\gamma| > u_L \text{ and } \dot{u}\beta < 0 \end{cases} \tag{24}$$

The position-limiting algorithm is applied whenever $|\alpha| \geq u_L$. Position limit activation is complicated by the fact that the velocity versus position envelope is a function of acceleration. That is, for any acceleration within the range ($\pm\ddot{u}_L$), the velocity may be displayed versus the position to determine an "area" of unrestricted travel excursions. The area is symmetric only for zero acceleration. For the vertical axis this is presented in Fig. 7. The parabolic limiting boundaries are shown for reference purposes.

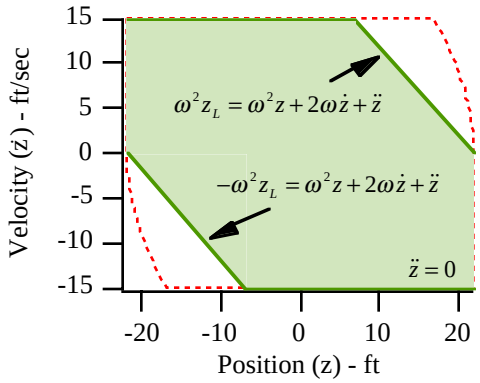

Fig. 7 – Zero Acceleration Boundaries

At a different acceleration the area is not symmetric. For positive acceleration, for instance, the boundaries of Fig. 7 (solid lines) are shifted downward, as shown in Fig. 8.

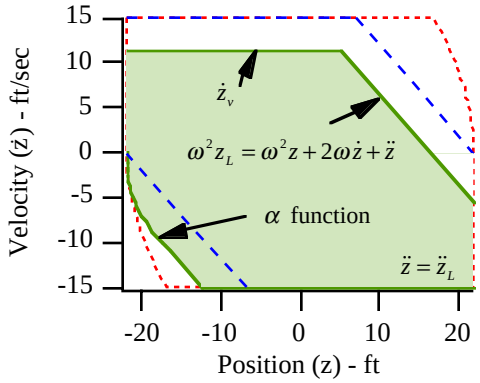

Fig. 8 – Maximum Acceleration Boundaries

The downward shift occurs until maximum acceleration is achieved, where the velocity limit decreases to the velocity breakpoint "$\dot{u}_v$". On the negative side the locus of boundaries becomes segmented into two sections (the α function), consisting of both a shifted, straight segment and a curved segment intersecting zero velocity when the position is at the negative limit. In the example of Fig. 8

the vertical acceleration is at the positive maximum limit. The parabolic boundaries are again shown for reference purposes. Also, the zero acceleration boundaries from Fig. 7 are reproduced as dashed lines.

As was shown in Fig. 6, at the velocity breakpoint $\dot{z}_v$ the velocity-limiting phenomenon occurs. Since the acceleration is positive in Fig. 8, the shifted velocity is limited on the negative side only by the hard limit. However, both velocity and position are curtailed due to position limiting, where the curve is shifted downward acquiring a curved component. For cases where the signs of both velocity and position are the same (while the sign of acceleration is opposite) this produces the α function, which is required to constrain all variables to their hard limits. For negative accelerations Fig. 8 would become its skew symmetric equivalent. This phenomenon produces volumes with up to 16 sides, representing the ROUTE for any given axis. Figs. 7 and 8 represented the *P*=0 case, which may be expanded to display the complete ROUTE (the entire acceleration range) by adding the acceleration dimension as in Fig. 9. Dividing this volume by the parabolic volume V_p results in an efficiency of 81.3% for the *P*=0 case.

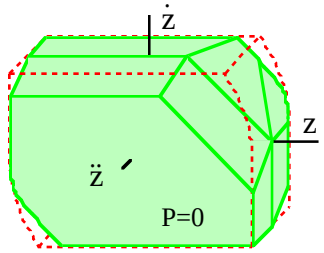

Fig. 9 – Vertical ROUTE, *P*=0, *E*=81.3%

When the normalized performance parameter is increased, a corresponding increase occurs in the ROUTE. Fig. 10 shows the case of *P*=1, where the efficiency becomes 93.3%.

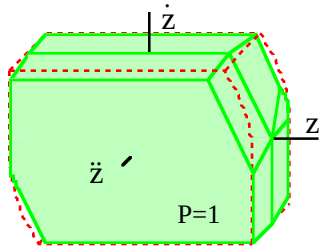

Fig. 10 – Vertical ROUTE, *P*=1, *E*=93.3%

X. Discrete Transition

Because nonlinear boundaries exist between regions, care must be taken in a discrete implementation to assure a robust solution. The triangular data hold is used in the discrete implementation of the washout filters because, besides the states u_k and $\dot{u}_k$, the acceleration $\ddot{u}_k$ must be computed. This is only an approximation using explicit algorithms such as the zero-order or first-order data hold because non-realizable (anticipative) forms for the acceleration are produced. Because the jerk is also an approximation, the acceleration must be accurate.

State transition methods are preferred for arbitrary washout filters, where seven coefficients λ_i are produced for a second-order system. They may be computed using a program called XFRSET (description and program listing available http://www.simlabs.arc.nasa.gov/) developed at Ames Research Center. This implementation of state-space software[5] is an example of techniques that have been used by the VMS facility for many years. The difference equations using the triangular data hold are given by,

$$\begin{bmatrix} u_k \\ \dot{u}_k \end{bmatrix} = \begin{bmatrix} \lambda_4 & \lambda_5 \\ \lambda_6 & \lambda_7 \end{bmatrix} \begin{bmatrix} u_{k-1} \\ \dot{u}_{k-1} \end{bmatrix} + \frac{1}{h}\begin{pmatrix} \lambda_1 \\ \lambda_2 \end{pmatrix} \ddot{x}_k + \left[\begin{pmatrix} \lambda_2 \\ \lambda_3 \end{pmatrix} - \frac{1}{h}\begin{pmatrix} \lambda_1 \\ \lambda_2 \end{pmatrix} \right] \ddot{x}_{k-1} \quad (25)$$

The acceleration is computed by use of the original differential equation in discrete form.

$$\ddot{u}_k = \ddot{x}_k - a_2\dot{u}_k - a_1 u_k \quad (26)$$

These equations are valid for the triangular data hold formulation. The state transition method delivers very efficient code for the computation of position, velocity, and acceleration. The four constant coefficients are defined,

$$\begin{bmatrix} \gamma_1 \\ \gamma_2 \\ \gamma_3 \\ \gamma_4 \end{bmatrix} = \begin{bmatrix} \lambda_1/h \\ \lambda_2/h \\ \lambda_2 - \gamma_1 \\ \lambda_3 - \gamma_2 \end{bmatrix} \quad (27)$$

Using these coefficients the entire real-time workload for state transition is given by the two equations,

$$\begin{bmatrix} f_{k-1} \\ g_{k-1} \end{bmatrix} = \begin{bmatrix} \lambda_4 u_{k-1} + \lambda_5 \dot{u}_{k-1} + \gamma_3 \ddot{x}_{k-1} \\ \lambda_6 u_{k-1} + \lambda_7 \dot{u}_{k-1} + \gamma_4 \ddot{x}_{k-1} \end{bmatrix}$$

$$\begin{bmatrix} u_k \\ \dot{u}_k \\ \ddot{u}_k \end{bmatrix} = \begin{bmatrix} \gamma_1 \ddot{x}_k + f_{k-1} \\ \gamma_2 \ddot{x}_k + g_{k-1} \\ \ddot{x}_k - a_2\dot{u}_k - a_1 u_k \end{bmatrix} \quad (28)$$

The zero order data hold is appropriate for both position and velocity limit filters because it delivers exact answers for constant inputs. The discrete solutions for the position-limiting and velocity-limiting filters are as shown in Fig. 11. All "λ" coefficients may be obtained from subroutine XFRSET.

Figure 11 displays the limiting algorithms applicable for any axis of motion. The "pseudo command" technique is used for a seamless interface between the various blocks.

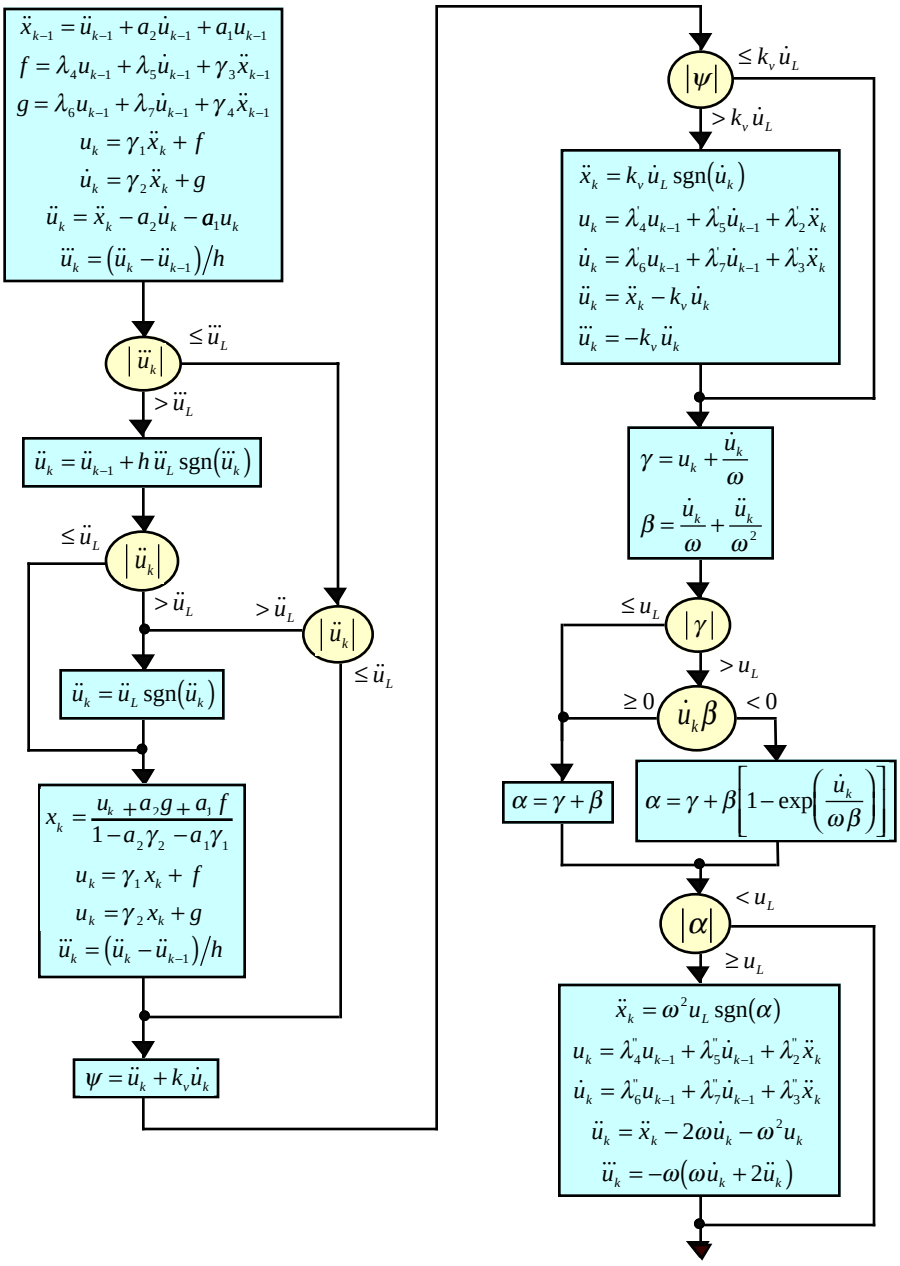

FIG. 11 – ALARMS DISCRETE MODEL

XI. Output Examples

Large amplitude pulse inputs can exercise all the limiting algorithms. This is especially true when the washout coefficients are zero, representing a one-to-one motion configuration. Parametric curves using this configuration are presented in Fig. 12 with four values for the performance parameter. When the pulse input occurs, the washout filter calls for the maximum acceleration of 22 ft/sec^2. This acceleration does not occur immediately, however, because of the jerk limit, which impacts trajectories most significantly for low parameter values. The slope due to jerk limiting is most significant in Fig. 12(a), where P=0.

The acceleration begins decaying when the velocity-limiting differential equation is activated. This is a slow decrease in Fig. 12(a) because P=0, and a rapid decrease in Fig. 12(d) because P=1. Similarly, when the position limiting differential equation is active the trajectories are

affected in accordance with the performance parameter, as previously shown in Figs. 2 and 3.

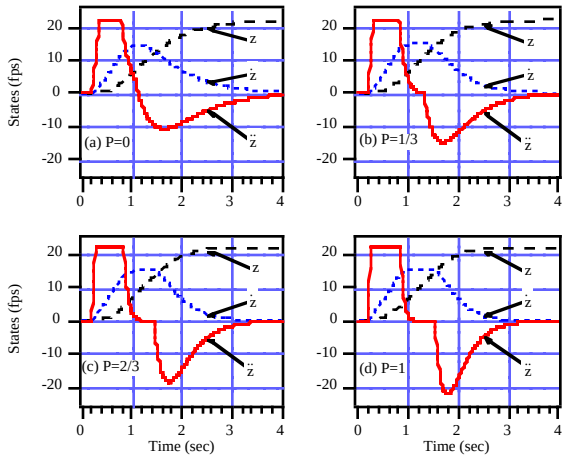

Fig. 12 – Pulse Input

The different trajectories during limiting are due to the performance parameter, where different values specify different permitted values of maximum jerk. The jerk histories for the four examples of Fig. 12 are given in Fig. 13.

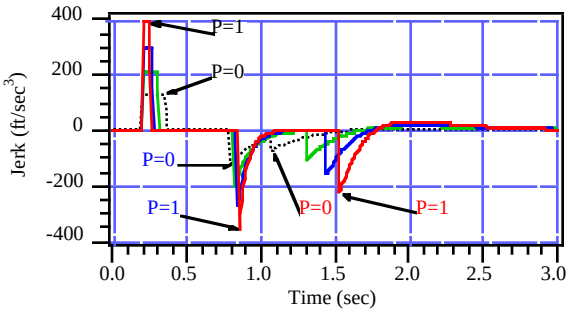

Fig. 13 – Jerk Histories

As a function of the performance parameter, jerk achieves its permitted maximum values at the pulse onset time. The arrow pointers in Fig. 13 (for the cases of *P*=0 and *P*=1) show three subsequent occurrences: (1) The termination of jerk limiting, where the acceleration finally achieves its maximum, (2) the onset of velocity limiting, and (3) the onset of position limiting. The jerk magnitude is limited in accordance with the value for *P* in each case, and the onset of limiting occurs at different times due to the decision logic.

XII. Improvements

The ALARMS system has been developed in order to:

- Simplify and quantify the limiting processes, and make them robust and "fail-safe."
- Establish a procedure for researchers and pilots to select the intensity of dynamics during limiting, thereby controlling the size of the "region of unrestricted travel excursions" (ROUTE).
- Optimize the ROUTE (and hence the efficiency) by determining the maximum locus of onset states for each limiting algorithm.
- Implement "jerk limiting" to minimize wear and tear on mechanical components as well as pilots.
- Create autonomous limiting procedures, where limiting (for each axis) is controlled by the selection of a single performance parameter.
- Implement position-limiting procedures for the case where both the position and velocity have the same sign, while the acceleration has the opposite sign.

The robust design of the ALARMS system is in anticipation of cueing algorithms that may further tax the capacity of a motion system, *e.g.*, "second-order mass-spring-dashpot operator cascaded with a first-order lead operator."[6] Increased performance of washout filters increases the probability of encountering unusual motion system states.

With respect to the original VMS system, ALARMS has produced the improvements in efficiencies shown in Figs. 14 and 15.

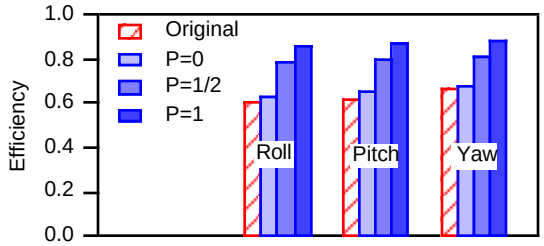

Fig. 14 – Rotation Efficiency

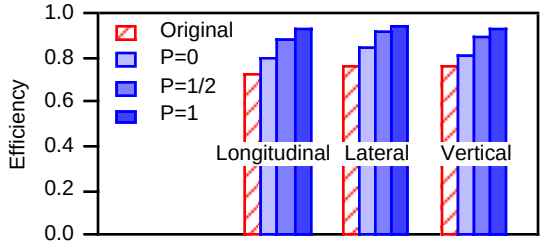

Fig. 15 – Translation Efficiency

The ALARMS system was implemented on the VMS late in 2000. As shown in Figs. 14 and 15 it is capable of increasing motion system efficiency by up to 30%, depending on the axis. As defined, this represents a

corresponding increase in the region of unrestricted travel excursions (ROUTE) - the region where washout filters are active, and simulation data are valid.

XIII. Conclusions

The optimal position-limiting filter is critically damped, with a unique natural frequency specified by the selection of a performance parameter. The parameter is directly related to the aggressiveness of motion cues during limiting, and the size of the "region of unrestricted travel excursions." Response magnitudes are quantified in terms of the maximum jerk that can be experienced during position limiting. The velocity-limiting filter is tuned to deliver the same maximum level of aggressiveness during its limiting procedures, and this limit is also used for the washout filters. These unifying restrictions create limiting algorithms and define metrics for the efficiency of a motion system. The performance parameter uniformly controls jerk during limiting up to adjustable maximums, and the motion system is generally constrained to its hard limits via trajectories much less aggressive than those of parabolic limiting.

The normalized parameter and resultant efficiency metric enable the research community to specify the per-axis simulator performance in terms of capacity and comfort. ALARMS constitutes a robust system that quantifies previously esoteric simulator performance boundaries, maximizes the available simulator capacity for normal operations, and assures that simulation experiments are not aborted by limit violations.

References

1. Advani, S.K. and Mebius, J.E.: "Determination of the Physical Volume of a Moving-Base Simulator," AIAA Modeling and Simulation Technologies Conference, AIAA-96-3375-CP, July 1996.
2. Advani, S. K., Nahon, M. A., Haeck, N., and Albronda, J.: "Optimization of Six-Degrees-of-Freedom Motion Systems for Flight Simulators," AIAA Modeling and Simulation Technologies Conference, AIAA-97-4504, August 1997.
3. Advani, Sunjoo Kan, "The Kinematic Design Of Flight Simulator Motion-Bases", Delft University Press, The Netherlands, 1998.
4. Wu, Weimin, and Cardullo, Frank M.: "Is There An Optimum Motion Cueing Algorithm?", AIAA Modeling and Simulation Technologies Conference, AIAA-97-3506, August 1997.
5. McFarland, R. E. and Rochkind, A. B., "On Optimizing Computations for Transition Matrices", IEEE Transactions on Automatic Control, Vol. AC-23, No. 3, June 1978.
6. Telban, Robert J., Cardullo, Frank M., and Guo, Liwen: "Investigation of Mathematical Models of Otolith Organs for Human Centered Motion Cueing Algorithms," AIAA Modeling and Simulation Technologies Conference, AIAA-2000-4291, August 2000.